

SUPPORTING INFORMATION

Hydrothermal Synthesis of Stable Lead-Free $\text{Cs}_4\text{MnBi}_2\text{Cl}_{12}$ Perovskite Single Crystals for Efficient Photocatalytic Degradation of Organic Pollutants

Xiao-Feng Qi,^a Fei Zhang,^a Zhi-Peng Chen,^a Xu Chen,^a Mo-Chen Jia,^a Hui-Fang Ji*^a and Zhi-Feng Shi*^a

^aKey Laboratory of Materials Physics of Ministry of Education, School of Physics and Microelectronics, Zhengzhou University, Daxue Road 75, Zhengzhou 450052, China

*Author to whom correspondence should be addressed. Electronic mail: shizf@zzu.edu.cn; jifang@zzu.edu.cn

EXPERIMENTAL SECTION

Materials. Cesium chloride (CsCl, 99.9%), anhydrous manganese chloride (MnCl₂, 99%), and bismuth trichloride (BiCl₃, 99.99%) were purchased from Sigma-Aldrich. Hydrochloric acid (HCl, analytical reagent) was purchased from Guangzhou Chemical Reagent Factory. Rhodamine B (RhB), Methylene Blue (MB), Sudan Red III were purchased from Shanghai Aladdin Biochemical Technology Co., Ltd. TEMPO was provided by Shanghai Macklin Biochemical Co., Ltd. All chemicals were used as received without further purification.

Synthesis of Cs₄MnBi₂Cl₁₂ Single Crystals. Cs₄MnBi₂Cl₁₂ single crystals were synthesized by hydrothermal method. In detail, the mixture of BiCl₃ (1 mmol, 315.34 mg), anhydrous MnCl₂ (1 mmol, 125 mg) and CsCl (4 mmol, 672 mg) were put into a mortar. After full grinding, the mixture was put into a 50 mL polytetraflurooroethylene (PTFE) container and HCl (10 mL) was added at the same time. After the mixture was completely dissolved, the container was sealed in a stainless-steel Parr autoclave and then placed in a drying oven and heated at 180 °C for 12 h. The temperature was subsequently lowered at a rate of 10 °C h⁻¹, and then the crystals of Cs₄MnBi₂Cl₁₂ were obtained. Finally, the obtained crystals were filtered out, washed with ethanol, and dried in vacuum at 80 °C overnight.

Photocatalytic Experiments. The test of photocatalytic reaction is carried out in the photochemical reaction instrument. In the presence of Cs₄MnBi₂Cl₁₂ SCs, the photodegradation of RhB, MB and Sudan red III ethanol solutions were carried out by 300 W mercury lamp at room temperature. Cs₄MnBi₂Cl₁₂ catalyst (5 mg) was mixed with 10 mL of RhB ethanol solution (10 mg/L), and then the mixture were stirred in the dark for 30 min to achieve adsorption-desorption equilibrium. We take out 4 mL of solution and use Shimadzu UV-3150 spectrophotometer to monitor the degradation rate of RhB through optical absorbance after 1 min of illumination. After the test is completed, we put the 4 mL of solution back into the reaction

tube to ensure that the volume of RhB solution is always 10 mL. It is worth noting that when monitoring the degradation rate of RhB, we need to place the whole reaction tube under dark conditions to ensure the strictness of the experiment. After another 1 min of illumination, take out 4 mL of solution for test, and repeat the previous operation until RhB is completely degraded. The signals of radical spin-trapped by spin-trap reagent DMPO were examined on the electron paramagnetic resonance spectra (EPR) at room temperature. The degradation products of RhB were determined by mass spectrometry.

Measurements and Characterizations. The microstructures of the as-synthesized $\text{Cs}_4\text{MnBi}_2\text{Cl}_{12}$ SCs were characterized by high-resolution transmission electron microscopy (TEM, JEOL, JEM-3010). The morphology and elemental composition of the samples were analyzed by a field-emission scanning electron microscope (SEM, JEOL JSM-7500F) and energy-dispersive spectroscopy (EDS, Oxford Instruments). The crystal structure of samples was characterized by X-ray diffractometer (XRD, Panalytical X’Pert Pro) with Cu Ka radiation ($\lambda = 1.5406 \text{ \AA}$). The absorption spectra of the samples were measured by ultraviolet-visible absorption spectrophotometry (Shimadzu UV-3150). The emission properties of samples were investigated using a steady-state photoluminescence (PL) spectra (Horiba, Fluorolog-3) and the transient-state PL was performed using a fluorescence lifetime measurement system with a pulsed nano-LED. The signals of radical spin-trapped by spin-trap reagent DMPO were examined on the electron paramagnetic resonance spectra (EPR, CIQTEK EPR200M) at room temperature. ^1H nuclear magnetic resonance (^1H NMR) spectra were recorded on a Bruker Advance III 400 MHz NMR spectrometer. The energy band properties were examined by ultraviolet photoelectron spectroscopy (UPS, EscaLab Xi+). The degradation pathway of RhB was analyzed by Ultimate 3000 UHPLC (Thermo Scientific, US).

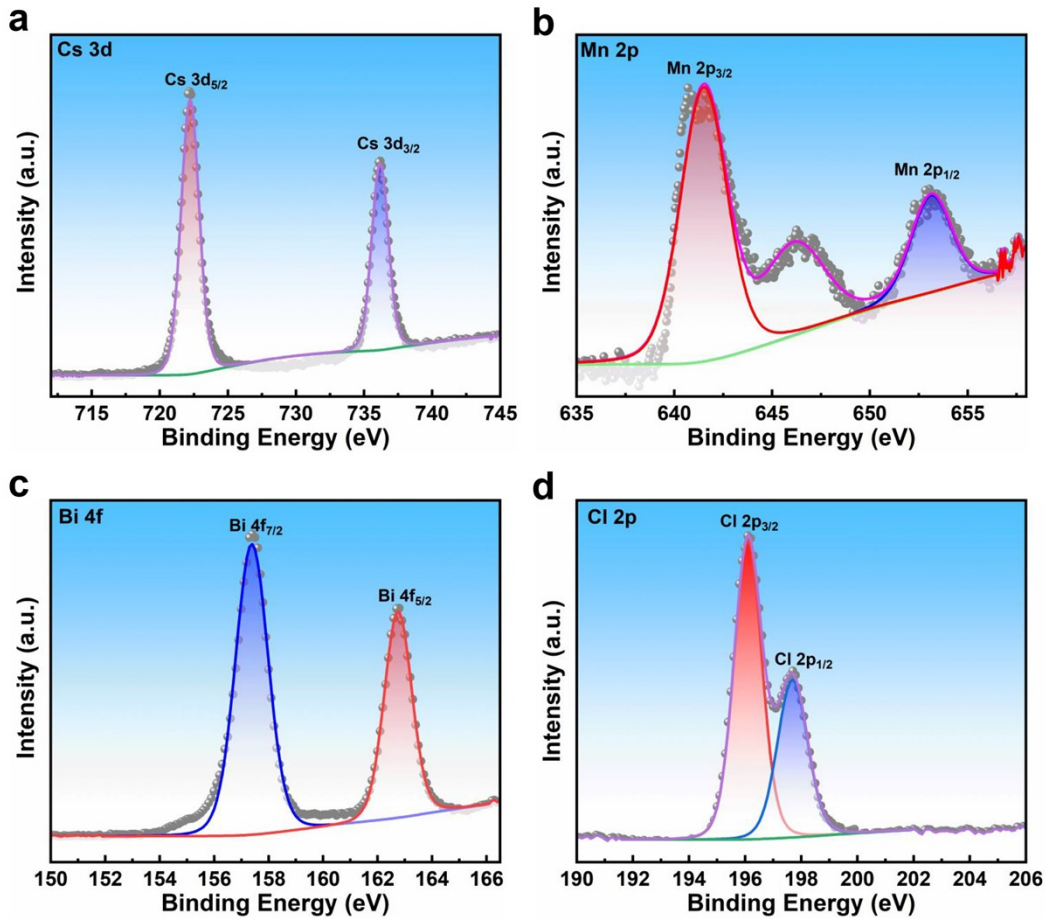


Figure S1. High-resolution XPS spectra of (a) Cs 3d, (b) Mn 2p, (c) Bi 4f, and (d) Cl 2p, respectively.

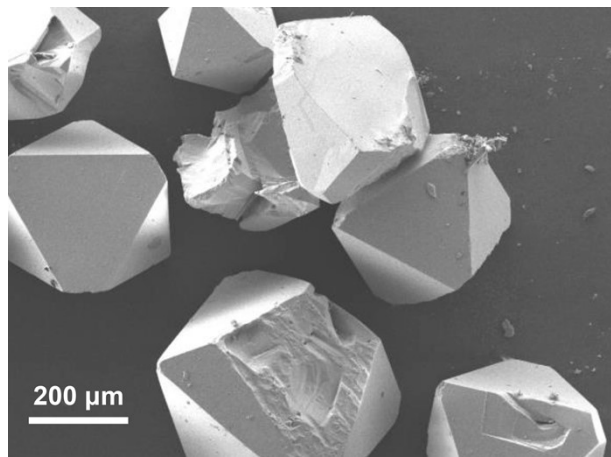


Figure S2. The low magnification SEM image of Cs₄MnBi₂Cl₁₂ single crystals.

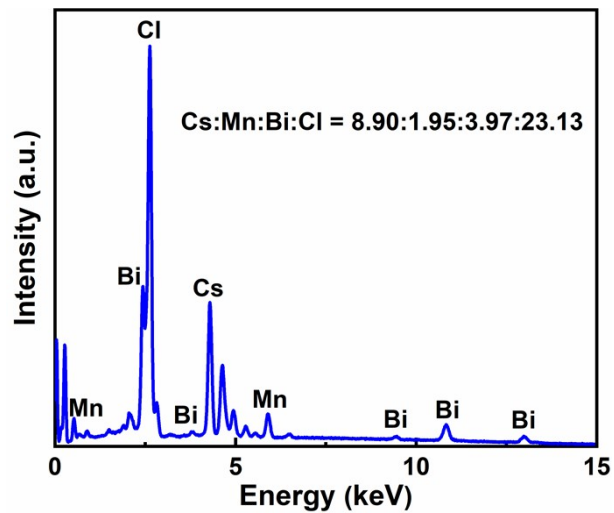


Figure S3. EDS spectrum and the composition analysis of $\text{Cs}_4\text{MnBi}_2\text{Cl}_{12}$ SCs.

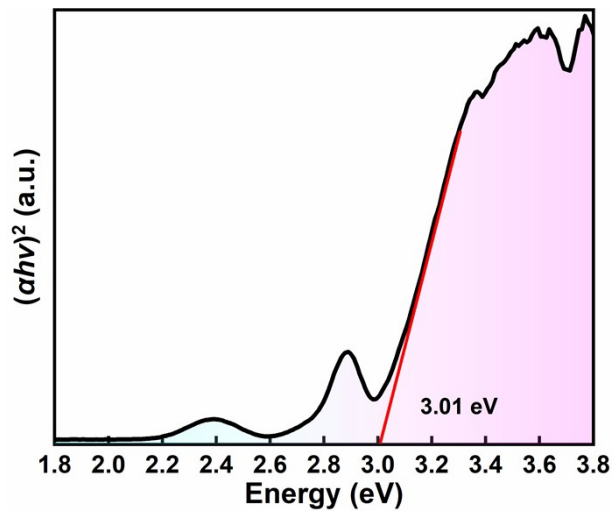


Figure S4. Tauc plots analysis of absorption spectrum of $\text{Cs}_4\text{MnBi}_2\text{Cl}_{12}$ SCs.

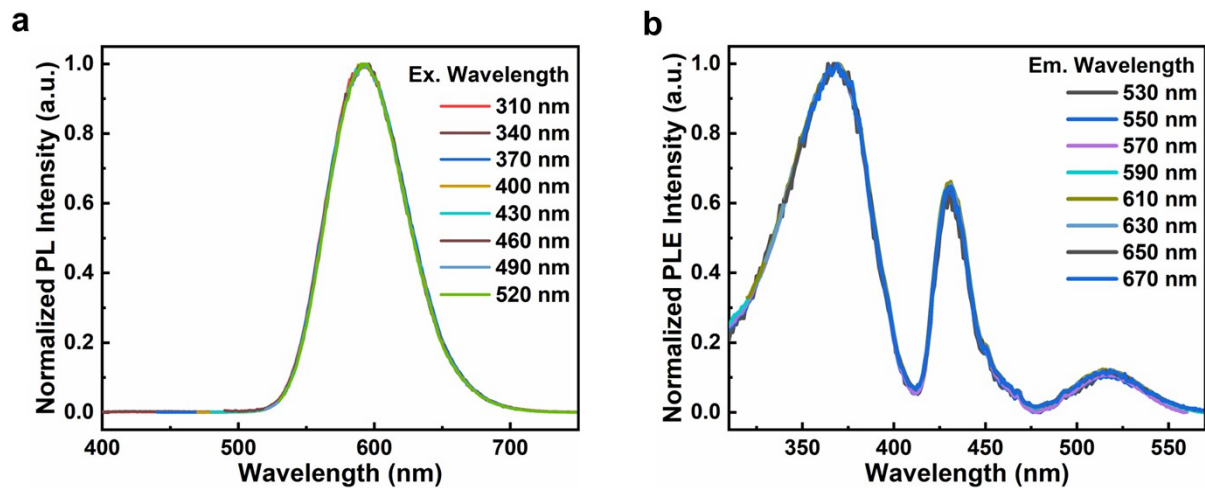


Figure S5. (a) Emission spectra of $\text{Cs}_4\text{MnBi}_2\text{Cl}_{12}$ SCs at various excitation wavelengths. (b) Emission-wavelength-dependent PLE spectra of $\text{Cs}_4\text{MnBi}_2\text{Cl}_{12}$ SCs.

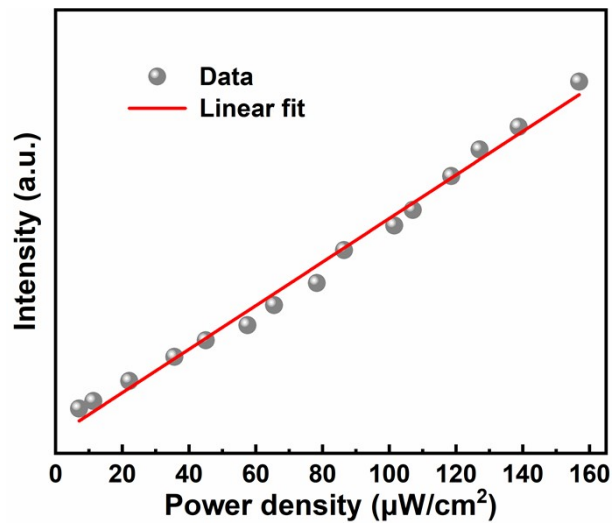


Figure S6. Dependence of PL intensity on the light power density of $\text{Cs}_4\text{MnBi}_2\text{Cl}_{12}$ SCs.

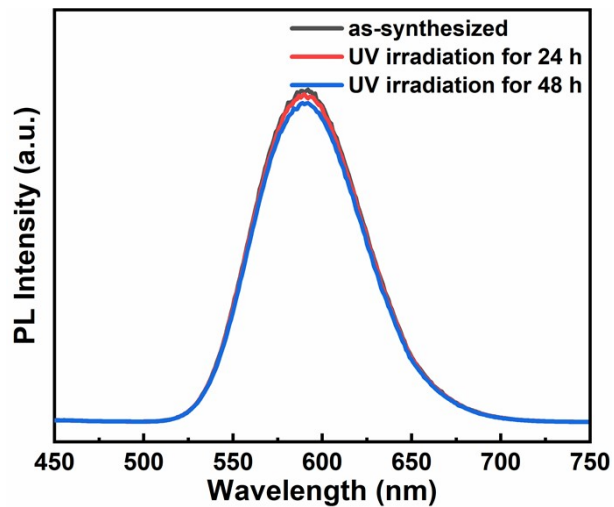


Figure S7. PL spectra of $\text{Cs}_4\text{MnBi}_2\text{Cl}_{12}$ SCs after continuous UV irradiation.

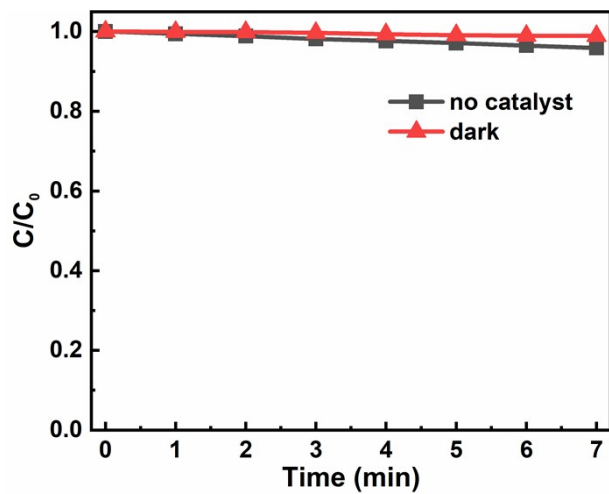


Figure S8. Plots of C/C_0 versus the irradiation time for the degradation of RhB without catalyst under light irradiation (red), and with catalyst under dark conditions (dark).

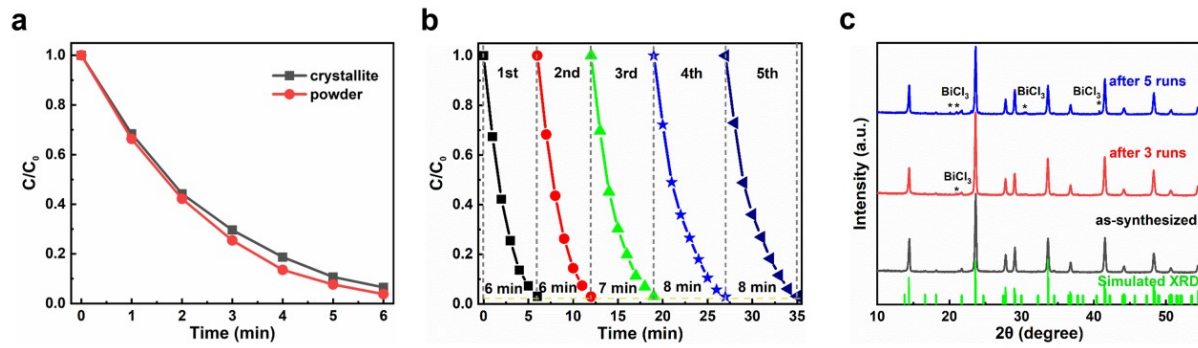
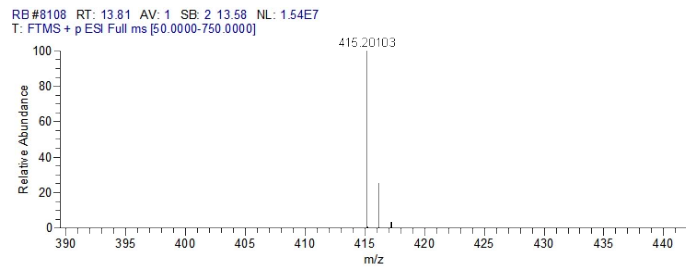
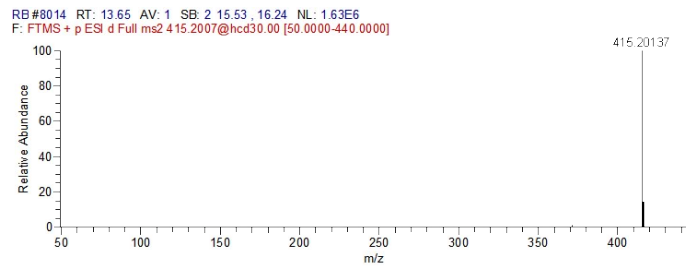
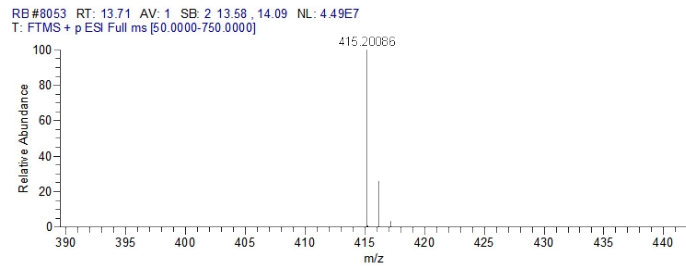
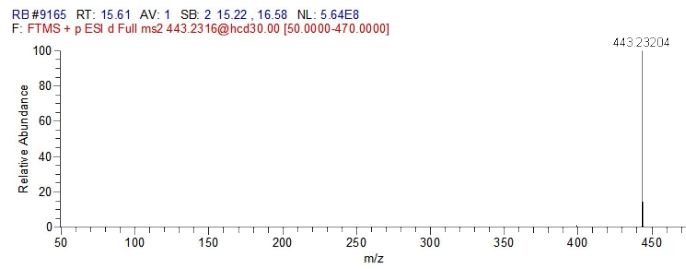
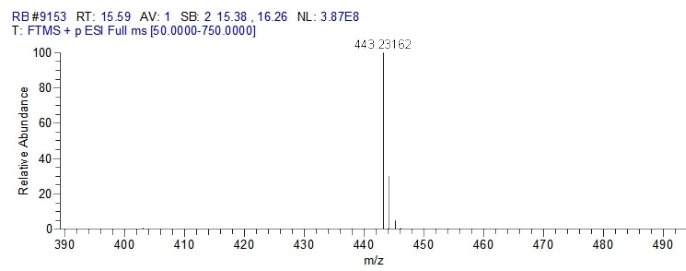
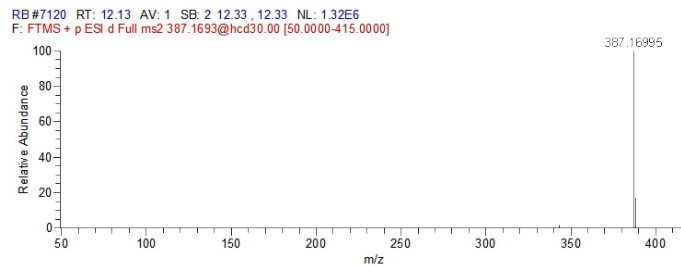
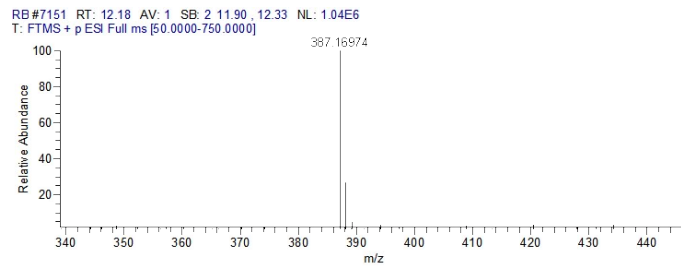
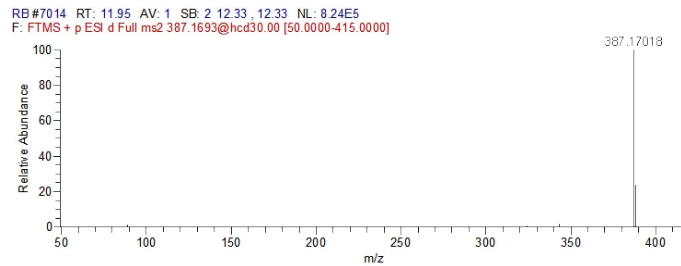
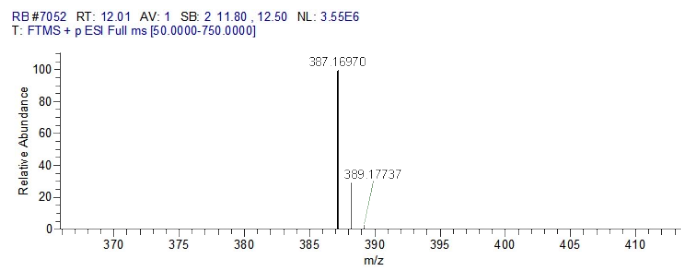
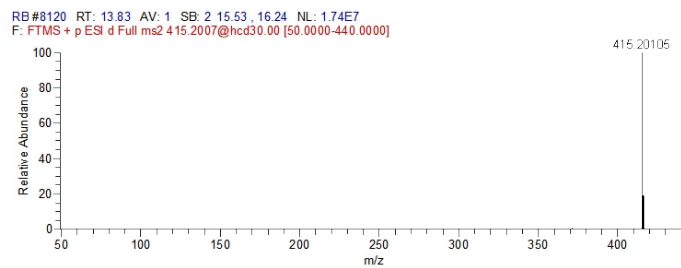
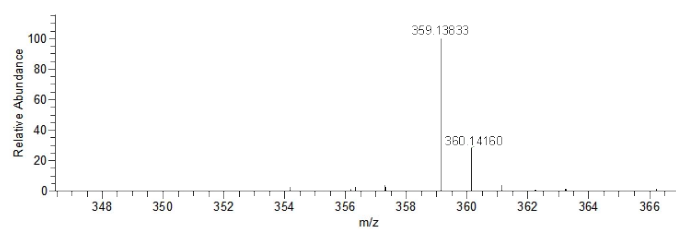


Figure S9. (a) Plots of C/C_0 versus the irradiation time for the degradation of RhB with $\text{Cs}_4\text{MnBi}_2\text{Cl}_{12}$ SCs and its powder. (b) Five degradation cycle tests of $\text{Cs}_4\text{MnBi}_2\text{Cl}_{12}$ powder under UV-light irradiation in photocatalytic degradation of RhB. (c) XRD patterns of $\text{Cs}_4\text{MnBi}_2\text{Cl}_{12}$ power before and after degradation cycle tests.

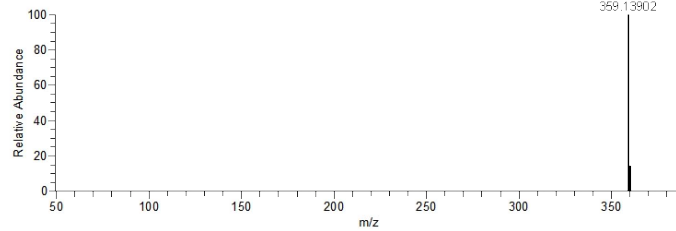




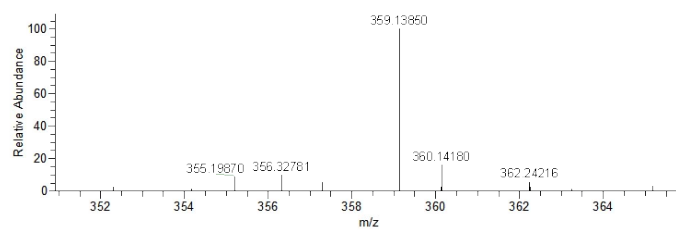
RB #6216 RT: 10.59 AV: 1 SB: 2 10.48, 10.90 NL: 1.15E6
T: FTMS + p ESI Full ms [50.000-750.000]



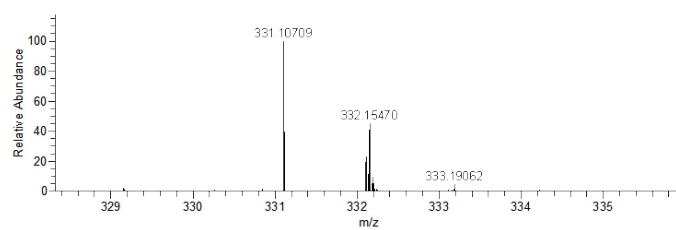
RB #6199 RT: 10.56 AV: 1 SB: 2 15.25, 15.25 NL: 1.64E6
T: FTMS + p ESI Full ms [50.000-385.000]



RB #6249 RT: 10.64 AV: 1 SB: 2 10.94, 10.46 NL: 4.63E5
T: FTMS + p ESI Full ms [50.000-750.000]



RB #5175-5608 RT: 8.83-9.54 AV: 39 SB: 2 8.96, 9.56 NL: 1.25E5
T: FTMS + p ESI Full ms [50.000-750.000]



RB #5385 RT: 9.18 AV: 1 SB: 2 18.59, 18.59 NL: 1.33E6
T: FTMS + p ESI Full ms [50.000-355.000]

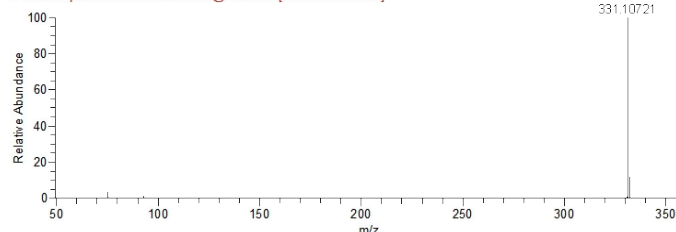
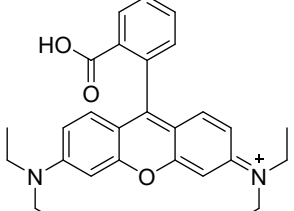
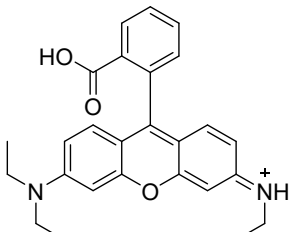
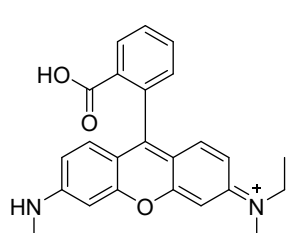
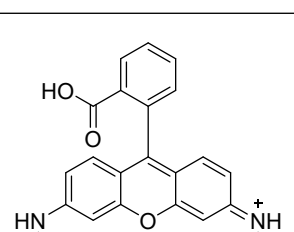
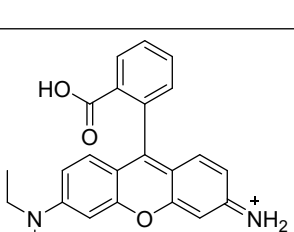


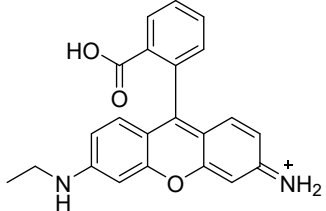
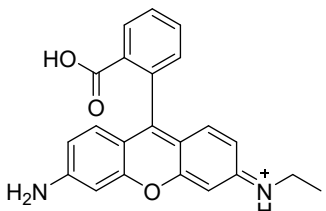
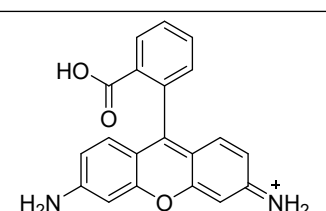
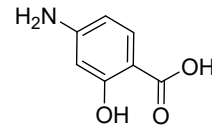
Figure S10. MS analysis of RhB after degradation using $\text{Cs}_4\text{MnBi}_2\text{Cl}_{12}$ SCs as a photocatalyst.

Table S1. Photocatalytic activity of perovskites-based photocatalysts for degradation of organic pollutants.

Photocatalysts	Contaminants	Concentrations (mg/L)	Time (min)	Cycle number	Degradation (%)	ref.
$\text{Cs}_2\text{AgBiBr}_6$	RhB	100	120	5	98	5
$\text{Cs}_2\text{AgInCl}_6$	Sudan Red III	10	16	5	98.5	6
$\text{Cs}_2\text{AgInCl}_6$	RhB	10	140	—	90.8	6
CsPbBr_3	MO	10	100	2	89	8
CsPbCl_3	MO	10	100	2	90	8
$(\text{CH}_3\text{NH}_3)_3\text{Bi}_2\text{I}_9$	RhB	20	180	3	98	9
$\text{Cs}_3\text{Bi}_2\text{Br}_9$	MB	20	100	2	99.3	10
$\text{Cs}_4\text{MnBi}_2\text{Cl}_{12}$	RhB	10	7	10	97	This work

Table S2. The reaction intermediates during RhB degradation determined by HPLC-MS analysis.

NO.	Molecular Formula	m/z	Name	Structural Formula
1	$C_{28}H_{31}N_2O_3^+$	443.2316	<i>Rhodamine B</i>	
2	$C_{26}H_{27}N_2O_3^+$	415.2008	<i>N-(9-(2-carboxyphenyl)-6-(diethylamino)-3H-xanthen-3-ylidene)ethanaminium</i>	
3	$C_{26}H_{27}N_2O_3^+$	415.2010	<i>N-(9-(2-carboxyphenyl)-6-(ethylamino)-3H-xanthen-3-ylidene)-N-ethylethanaminium</i>	
4	$C_{24}H_{23}N_2O_3^+$	387.1697	<i>N-(9-(2-carboxyphenyl)-6-(ethylamino)-3H-xanthen-3-ylidene)ethanaminium</i>	
5	$C_{24}H_{23}N_2O_3^+$	387.1697	<i>9-(2-carboxyphenyl)-6-(diethylamino)-3H-xanthen-3-iminium</i>	

6	$C_{22}H_{19}N_2O_3^+$	359.1383	<i>9-(2-carboxyphenyl)-6-(ethylamino)-3H-xanthen-3-iminium</i>	
7	$C_{22}H_{19}N_2O_3^+$	359.1385	<i>N-(6-amino-9-(2-carboxyphenyl)-3H-xanthen-3-ylidene)ethanaminium</i>	
8	$C_{20}H_{15}N_2O_3^+$	331.1070	<i>6-amino-9-(2-carboxyphenyl)-3H-xanthen-3-iminium</i>	
9	$C_7H_8NO_3^+$	139.0500	<i>4-amino-2-hydroxybenzoic acid</i>	
10	$C_7H_7O_3^+$	154.0496	<i>2-hydroxybenzoic acid</i>	